5.2 Meso-β scale precipitation systems evolved at Tsushima Straits during late Baiu season in 2009

Hirohisa Mizuno* and Kenji Tanaka*
*Department of Civil and Environmental Engineering, Kumamoto University, Kumamoto, Japan

1. Introduction

During late July in 2009, severe rainfall due to the baiu front caused much damage to the Chugoku and northern Kyushu district in Japan. As listed in Table 1, more than 30 people were lost by sediment disaster caused by heavy rainfall.

The record of ground rainfall observed by the Japan Meteorological Agency (JMA) in Figure 1 showed that the total rainfall from 21st to 26th July 2009 exceeded to 500 mm in the west of Chugoku district and in the north coastal area of the Kyushu district. The amount of rainfall of three days was 618.0mm in Dazaihu (Fukuoka), 568.0mm in Iizuka (Fukuoka) and 458.5mm in Gongenyama (Saga) from 0 in July 24th to 24 in July 26th, this amount of rainfall was double of the average precipitation in July. The distribution of hourly precipitation showed that the area of severe squall concentrated in the same area of the high accumulated rainfall. Especially, at the Fukuoka International Airport, the maximum hourly rainfall was recorded to 116.0 mm in the evening of 24 July 2009 (see Figure 2).

The infrared images by a geostationary meteorological satellite (MTSAT) showed that the mesoscale Cb cluster evolved continuously in the Tsushima Strait with the horizontal scale of tens to hundreds kilometers and reach for the approached Kyushu, as seen in Figure 3.

The past studies on baiu front system showed that the thermodynamic structure including atmospheric moisture plays an important role in the evolution of mesoscale disturbance (e.g., Moteki et al., 2004). However further detail of the structure of the precipitation system remains to be investigated, especially in the lowest atmosphere and the relation with the synoptic motions.

Therefore, this study is aimed to investigate the thermodynamic characteristics and structure of the meso-β scale systems and their surrounding synoptic scale systems.

* Corresponding Author, Address: Hirohisa Mizuno, Department of Civil and Environmental Engineering, Faculty of Engineering, Kumamoto University, Kurokami 2-39-1, Kumamoto city, Kumamoto, 860-8555, Japan; email: 06@st.kumamoto-u.ac.jp

Table 1 List of damage caused by the heavy rainfall in the late of baiu season

Personal Damages	Lost	31
	Wounded	46
Natural Disasters (cases) 66 cities	Avalanche of rocks and earth	76
	mudslide	347
	landslide	12

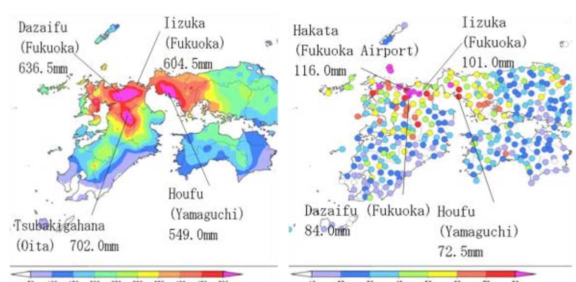

Figure 1 Distribution of ground rainfall from 21st to 26th July 2009, observed by Japan Meteorological Agency (JMA): the accumulated rainfall in the left panel and the maximum of the past 1-hour rainfall in the right panel.

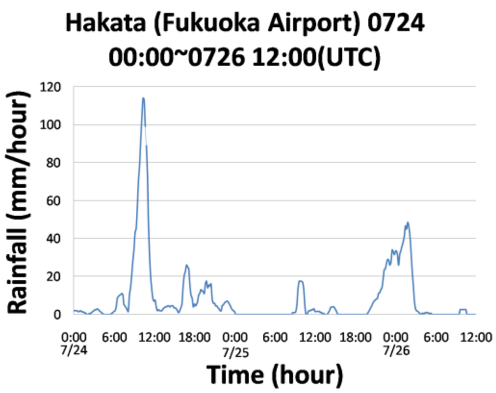

Figure 2 Past 1-hour rainfall observed at Fukuoka International airport

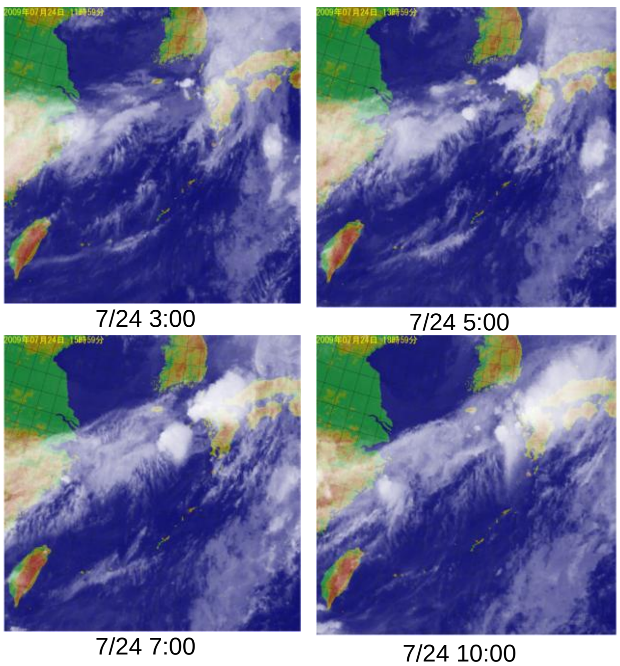

Figure 3 Images of MTSAT IR-1 channel during the daytime on 24 July 2009.

2. Datasets

The characteristics of the thermodynamic properties such as equivalent potential temperature and its gradient were investigated using the reanalysis by JMA, with the horizontal resolution of about 10 km for each isobars and of 5 km for surface, provided every 3 hours. It covers a whole of Japan and the East China Sea. The horizontal wind, vertical velocity in pressure variation, temperature and relative humidity (lower than 250 hPa) were included in the reanalysis dataset.

3. The structure of mesoscale disturbance in the Tsushima Strait

Figure 4 shows the difference between the temperature and dew point temperature (T-Td) at 700hPa in July 24 and height at 500hPa. In this figure, the trough meandering and go south to the East China Sea is stationary. The dry air mass trapped this trough is on the Shanghai to the Yellow Sea., The moist air mass from the China continent is in the east side of this dry air mass. So, the gradient of vapor has developed between the dry air mass and the moist air mass.

Figure 5 shows the equivalent potential temperature (EPT) at 1000hPa 7/24 00UTC. In this figure, there is the area of crowded contour of EPT from Cheju Island to Tsushima, and especially, the line is kinked up to north in latitude 34 degrees north and longitude 129 degrees east. In this area, the difference of EPT is more than 20K (in the south side of the kink, the EPT is more than 350K, and the north side is 330K); in the north side, there is strong stream of hot and moist air from the East China Sea, in the north side, the wind from ENE is strong, and these streams make up the horizontal shear of wind. In this baroclinic instability developed by the kink of EPT toward north, the meso low whose diameter is from100 to 200km occurred and moved to east. Also, the south east area of high EPT from this low toward south west is

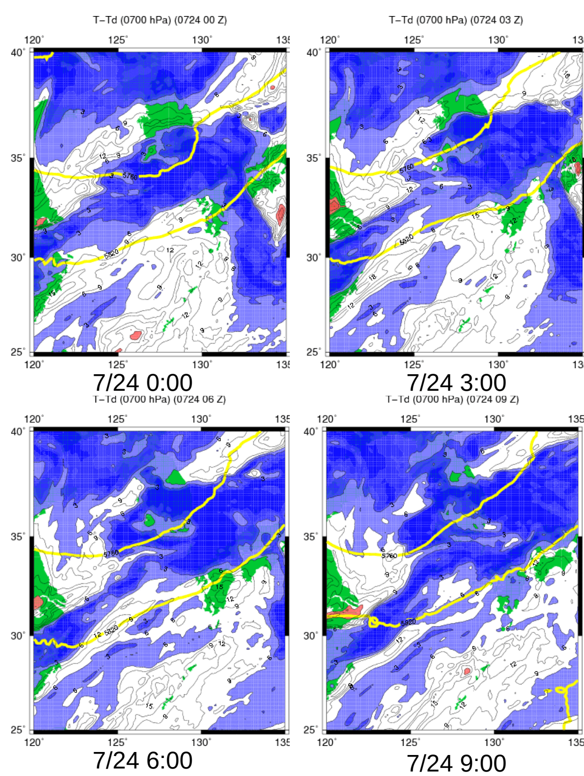

Figure 4 Distribution of T-Td at 700hPa and 500hPa geopotential height

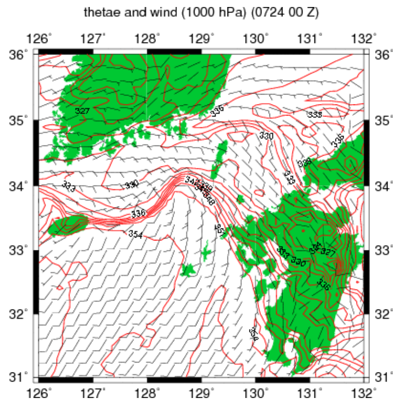

Figure 5 EPT at the lowest atmosphere (1000hPa), with branch of wind barb every 5m/s

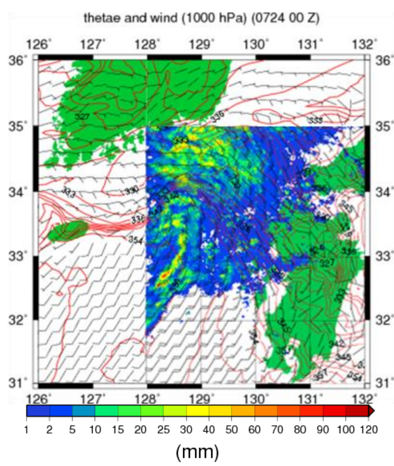

Figure 6 Similar as Figure 5 but radar echo intensity was overlaid

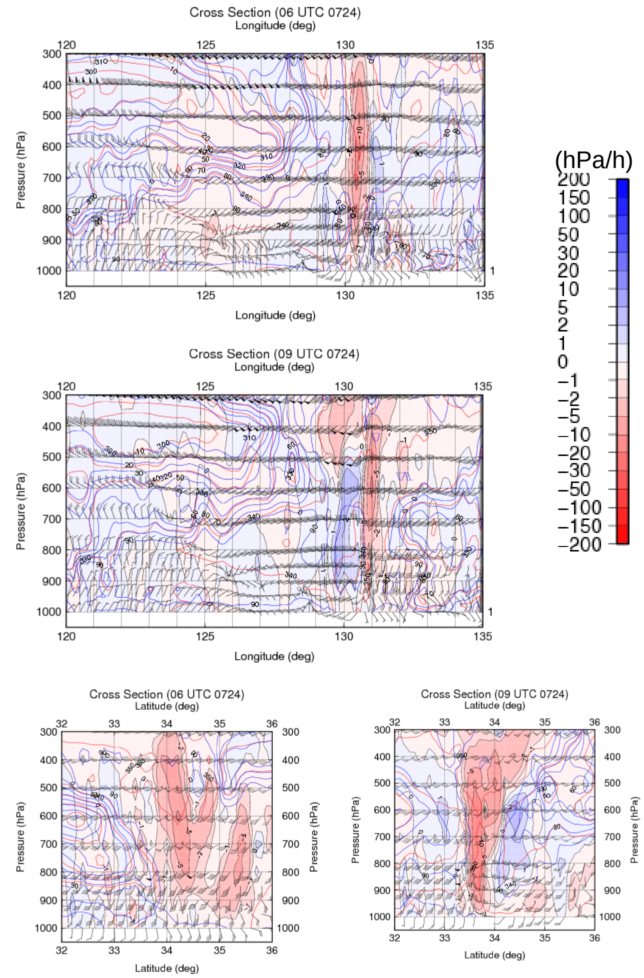

Figure 7 Vertical cross section of EPT, RH and vertical velocity ω.

almost equal to the area of heavy rainfall observed by the meteorological radar (Figure 6).

As to the crowed area of EPT, we took the vertical cross section and surveyed the relation to wind area. Figure 9 shows the results. The EPT line is red, the relative humidity (RH) line is blue and back ground color is p-velocity (ω). In the E-W cross section 7/24 00UTC, the dry air mass which has low EPT and RH is west of the longitude 125 degrees east, and in this area, we can see the downward flow in the large region. Also, there is the strong upward flow, correspond to the kink of EPT line. While the N-W wind can be seen in the area of dry air entering, in the area of upward flow, the strong wind can be seen from S-W by the 300hPa.

On the other hand, taking the S-N cross section, the area seen the upward flow in the latitude from 34 to 35 degrees north at 06UTC went south in the latitude about 33 degrees 40 minutes north at 09UTC, and this area correspond to the area of the heavy rainfall observed by radar. According to the satellite image, we can see the crowds spreading south and north toward east, and this area correspond to the area of upward flow at 300hPa spreading in the latitude from 33 to 35 degrees north.

4. Influence of the synoptic scale motion using WRFV3

To solve the mechanism of sever precipitation system. We need the data of large scale. But the global data by NCAR or JMA is rough of these horizontal resolutions. Hence, in this study, we used the numerical model, Weather Research and Forecast (WRF) to analyze the detailed system. Table 2 lists the condition of calculation of WRF and Figure10 shows the area of calculation. For the initial and four dimensional data assimilation, JMA GSM (Global Spectrum Model) reanalysis data and NCEP SST (Sea Surface Temperature) were used.

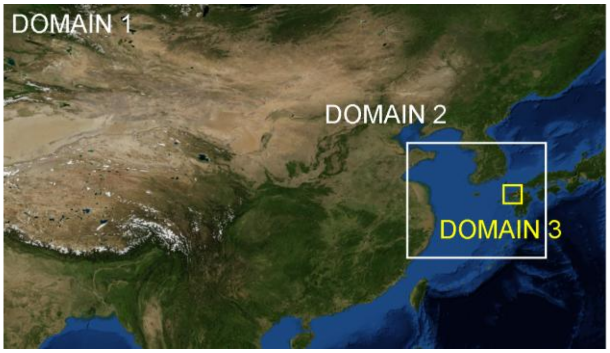

Figure 8 Area of calculation of WRF.

Table 2 Condition to calculate of WRF.

Domain	1	2	3
number of grid (nx x ny)	150 x 90	161 x 136	109 x 101
Horizontal spacing	~ 40 km	~ 8km	~ 2km
Start and forecast time	7/22 00Z + 96hr	7/23 00Z + 72hr	7/23 12Z + 48hr
Grid FDDA	on	on	off
Cumulus parameteri-zation	Kain-Fritcsh scheme	Kain-Fritcsh scheme	None

Figure 9 shows the distribution of cyclonic circulation with the vorticity 3.0×10^{-5} s^{-1}, in which the color indicates the mixing ratio on the isosurface. Arrows show the streamline calculated from steady flow. In the upper atmosphere from the Tibetan Plateau to Japan, the area of cyclonic circulation went around the northern side of the highland and meandered to south from Beijing to northern Kyushu. In the middle China Plane the east side of the highland, the air mass going around the north side of the highland went south and down to lower layer, and the moist air mass going around the south side of the highland went north. So the belt of converge was made up, the area of positive vorticity developed at the middle-lower troposphere. Corresponding to the positive vorticity area in the north side, the dry air mass was transported continuously along the trough.

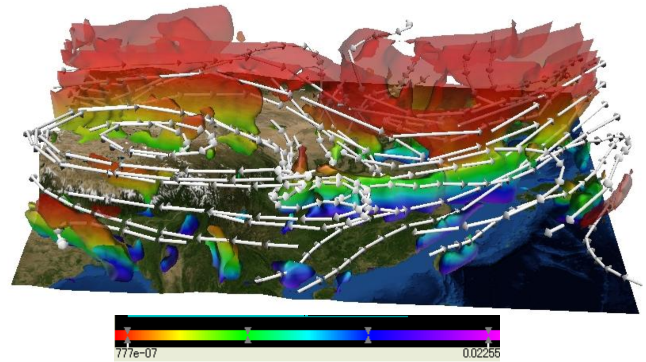

Figure 9 Distribution of cyclonic circulation with the vorticity 3.0×10^{-5} (1/s) over the east asia region (at 00Z 24 Jul 2009) after computed by WRFV3. Color on the isosurface indicates the mixing ratio

5. Conclusion

In this study, we analyzed the heavy rainfall system occurred at northern Kyushu in 24 July 2009.In the middle troposphere, the dry air mass was trapped inside the trough above the Yellow Sea. At the lowest atmosphere, the continental and oceanic moist air mass had been grown and joined at the coastal area of the northwest Kyushu. The kink of the vapor front occurred at the middle of the Tsushima Straits, which associated with the evolution of the tapering clouds. As to the convection above the vapor front, we found the maximum area of the Jet at the atmosphere equivalent to the Level of Free Convection, so the Jet play a important role to spread this convection latitudinaly.

References

Kato, T., 2006: Structure of the band-shaped precipitation system inducing the heavy rainfall observed over northern Kyushu, Japan on 29 June 1999. *J. Meteor. Soc*. Japan, **84**, 129-153.

Kato *et al*., 2003: Reason for the failure of the simulation of heavy rainfall during X-BAIU-01. –Importance of a vertical profile of water vapor for numerical simulations-. *J. Meteor. Soc*. Japan, **81**, 993-1013.

Matsumoto *et al*., 1971: Characteristic features of Baiu front associated with heavy rainfall. *J. Meteor. Soc.* Japan, **49**, 267-281.

Moteki et al., 2004: Structure and development of two merged rain bands observed over the East China Sea during X-BAIU-99: Part II: Meso-α-scale structure and build-up processes of convergence in the Baiu frontal region. *J. Meteor. Soc.* Japan, **82**, 45-65.